Benha Journal of Applied Sciences (BJAS) **print: ISSN 2356–9751**
Vol. (10) Issue (4) (2025), (79- 88) **online: ISSN 2356–976x**
http://bjas.bu.edu.eg
engineering sciences

Performance and Emissions Analysis of a Single-Cylinder CI Engine Operated with Diesel and HHO Gas Produced by a Dry Cell Electrolyzer

Mahmoud Aboukhalifa [1], Ahmed I.EL-Seesy [1,2], A.A.Hawwash [1,3] and A.S.Huzayyin [1]
[1] Mechanical Engineering Dept., Benha Faculty of Engineering, Benha University, Benha 13512, Egypt.
[2] Mechanical and Nuclear Engineering Dept., College of Engineering and Physical Sciences, Khalifa University, Abu Dhabi 127788, United Arab Emirates.
[3] Graduate School of Science and Engineering, Institute of Science Tokyo, Tokyo, Japan.
E-mail: mahmoud.khaled@bhit.bu.edu.eg.

Abstract
Research and investment in renewable energy are vital for a sustainable future to meet the growing global energy demand driven by worldwide population growth. Dependence on fossil fuels contributes to environmental degradation and resource depletion. Renewable energy sources, such as hydrogen, have been proven to offer a sustainable alternative that reduces emissions and enhances energy security. However, hydrogen gas faces storage challenges and potential hazards. Oxyhydrogen gas (HHO), produced onboard without storage, provides a viable alternative. HHO, a mixture of hydrogen and oxygen generated via water electrolysis, was utilized in this study. The research aimed to design and implement a dry cell HHO generator to supply a steady 0.25 LPM flow rate into a single-cylinder CI engine. HHO gas was introduced through a drilled port at the intake manifold. The performance and emissions of the dual-fuel engine, powered by Diesel and HHO, were analyzed. Results showed improved brake thermal efficiency and reduced brake-specific fuel consumption with HHO integration. Emission data revealed significant reductions in carbon monoxide (CO), nitrogen oxides (NO_x), and unburned hydrocarbons (UHC), particularly at higher engine loads. Higher HHO flow rates were recommended to be tested to determine the optimal enrichment ratio for the engine's volume.

Keywords: HHO; Diesel; Dry cell; Performance; Emissions.

1. Introduction

The need for energy is increasing due to the expansion of the global population. Climate change and other environmental issues are caused by emissions from the combustion of fossil fuels [1]. Hence, alternative sustainable energy resources were investigated, such as wind, solar, and hydrogen energy. Hydrogen energy is considered one of the promising renewable energy resources that could help tackle the energy issue and global warming [2][3]. A principal advantage of using hydrogen in fuel cells is the absence of greenhouse gas emissions, as its combustion yields only pure water as a byproduct. Hydrogen is easily transported and stored, becoming an outstanding resource of energy for many applications, such as internal combustion engines [4]. Hydrogen is a decent energy carrier as it possesses a high calorific value and does not emit carbon-based emissions when burned. However, hydrogen production and storage can be expensive and challenging, which has led to the move to alternative hydrogen production methods. One such method is the use of HHO gas, which is identified as oxyhydrogen gas and consists of a hydrogen and oxygen mixture generated by the simple electrolysis of water [4]. Water is split to produce HHO gas by passing a current through the electrolyte solution [5]. HHO gas can be used in many applications. It is applicable in metal cutting, welding, power generation in gasoline and diesel engines as an enrichment fuel, domestic uses, and the removal of carbon gum residuals from engine and vehicle components, including spark plugs, pistons, fuel injectors, and catalytic converters [6].

There are two types of HHO gas electrolyzers: wet cell and dry cell, which are distinct in terms of their design and operation. Wet cell HHO electrolyzers use charged anode and cathode plates immersed in the electrolyte solution, typically KOH or NaOH dissolved in distilled water, to pass an electric current between two electrodes. The material of the electrodes is stainless steel 316L, which is more corrosion resistant, and the electrolyte is continuously recirculated to reduce overheating and gas buildup in the cell. HHO gas productivity of wet cells is usually higher than dry cells due to the full immersion of the plates in the liquid electrolyte, which enhances the conductivity and accelerates the electrolysis process [7]. However, wet cell electrolyzers need more maintenance because the electrolyte liquid solution should be frequently replaced, and the cells should be cleaned regularly to stop impurity buildup. Conversely, for dry cells, an electrolyte is controlled inside rubber gaskets separating the plates, so the plates are not fully immersed in the solution; hence, dry cells create less heat, cause less electrode plate corrosion, and are more compact than wet cells, so they are more practical and beneficial [7][8].

El Soly et al. [9] discussed the various parameters that affect the HHO gas production from cells. It was shown that increasing either the applied current, electrolyte concentration, cell gaps, or cell temperature caused an increase in the HHO productivity rate. A literature review for using HHO gas as an enrichment fuel for compression ignition (CI) engines fueled by diesel as a base fuel is summarized in Table 1.

Based on prior research in this field, there is no universally established optimal ratio for supplying

HHO gas to compression ignition (CI) engines. Previous studies have employed a wide range of flow rates, yielding inconsistent and sometimes contradictory outcomes. The present study focuses on designing and implementing HHO dry cell electrolyzers, followed by a comprehensive evaluation of the performance and emission characteristics of a CI engine fueled by diesel supplemented with a modest HHO gas flow rate of 0.25 liters per minute (LPM). This investigation seeks to determine whether this specific ratio significantly improves engine performance and emissions. Based on the findings, recommendations for future research directions are proposed to explore further the potential benefits and limitations of HHO gas integration in CI engines.

Table 1 Literature review of introducing HHO gas into CI engines.

Author(s)	Engine Specs.	HHO rate	Performance	Emissions
Thangaraj and Govindan [10]	Kirloskar AV1 $V_d = 553\ cm^3$ Single Cylinder Water cooled 3.7 kW at 1500 rpm	0.73 LPM	BTE ↑ by 19.66%. BSFC ↓ by 15.9%.	NO_x ↓ by 2.44%. CO ↓ by 11.2%. UHC ↓ by 34.6%. Smoke opacity ↓ by 44.83%.
Gad and Abdel Razek [11]	HATZ-1B30-2 Single cylinder. Air cooled 5.4 kW at 1500 rpm	Not mentioned	BTE ↑ by 2.5%. EGT ↓ by 10%.	CO ↓ by 22%. UHC ↓ by 39%. NO_x ↓ by 42%. Smoke ↓ by 35 %.
Liu et al. [12]	186F. $V_d = 406\ cm^3$ 5.7 kW at 3000 rpm	2 LPM	___	CO ↓ by 22.2%. UHC ↓ by 11.33%. PM ↓ by 20.71%. NO_x ↑ by 9.5%.
Abbas Gohar and Raza [13]	TQ200 Single Cylinder. $V_d = 232\ cm^3$ 3.1 kW at 3000 rpm.	5 LPM	BSFC ↓ by 27%. BP ↑ by 22% BTE ↑ by 47%.	___
Manu et al. [14]	Kirloskar. $V_d = 553\ cm^3$ Single Cylinder 5 hp at 1500 rpm	0.89 LPM / 1.37 LPM / 1.66 LPM / 2 LPM	BTE ↑ by 34.99% max. BSFC ↓ by 7.8% max.	CO_2 ↓ by 8.9% max. NO_x ↑ by 9.7% max.

2. Materials and methods

2.1. Test fuels

HHO gas was generated from a 4-cathode, 4-anode, 28-neutral plates (4C4A28N) dry cell. Anode, cathode, and neutral plates were CNC cut from a 1 mm-thick 316L stainless steel sheet. Neoprene rubber of 3 mm thickness was cut and used as a gasket to separate the successive plates and contain the electrolyte solution to conduct the electric current. The electrolyte solution concentration for this experimental program was 20 g/L of NaOH dissolved in distilled water using a magnetic stirrer for ten minutes. These components of the dry cell were assembled with screws and 8 mm thickness clear acrylic end plates.

The schematic diagram in Figure 1 shows the other components of the HHO generator rather than the dry cell itself, where it is connected to a 12V and 30A DC power supply, an electrolyte reservoir for electrolyte compensation and primary gas separation, a bubbler to separate HHO gas and act as a water barrier to prevent flashbacks, a pulse width modulation (PWM) controller to control the HHO productivity rate by controlling the width of the duty cycle and hence controlling the power consumed, an ammeter, a voltmeter, and a thermometer. This HHO dry cell electrolyzer could generate a maximum flow rate of 1.75 LPM of HHO at full load. The oxyhydrogen rate used in the test was kept fixed at 0.25 LPM.

Neat diesel fuel purchased from a local gas station was used to run the engine as a primary fuel, whereas HHO was introduced to the air intake manifold as an enrichment fuel, as will be discussed in the following section. The properties of the used fuels are listed in Table 2. The thermal gravimetric analysis of the used diesel exposed in Figure 2 (a) reveals the weight loss of diesel over a range of temperatures, marking the bulk weight loss to be over the range between 140 ˚C to 350 ˚C, on the other hand, Figure 2 (b) shows the rate of that weight loss marking a maximum weight loss rate of 25.6 mg/min at 293 ˚C.

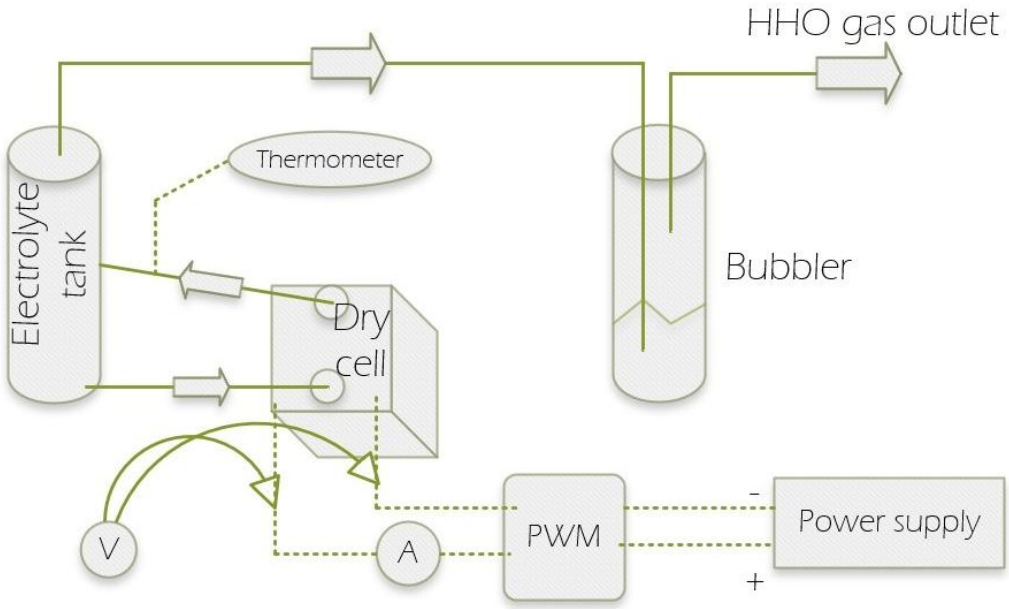

Fig. 1 A schematic diagram for the HHO generator.

Table 2 Tested fuels' properties.

Property	Diesel	Oxyhydrogen (HHO)[15]
Density (kg/m^3)	827.7	0.49
Heating value (MJ/kg)	42.49	21.99
Cetane number (CN)	46	53.3
Kinematic viscosity (mm^2/s)	3.4	0.0009

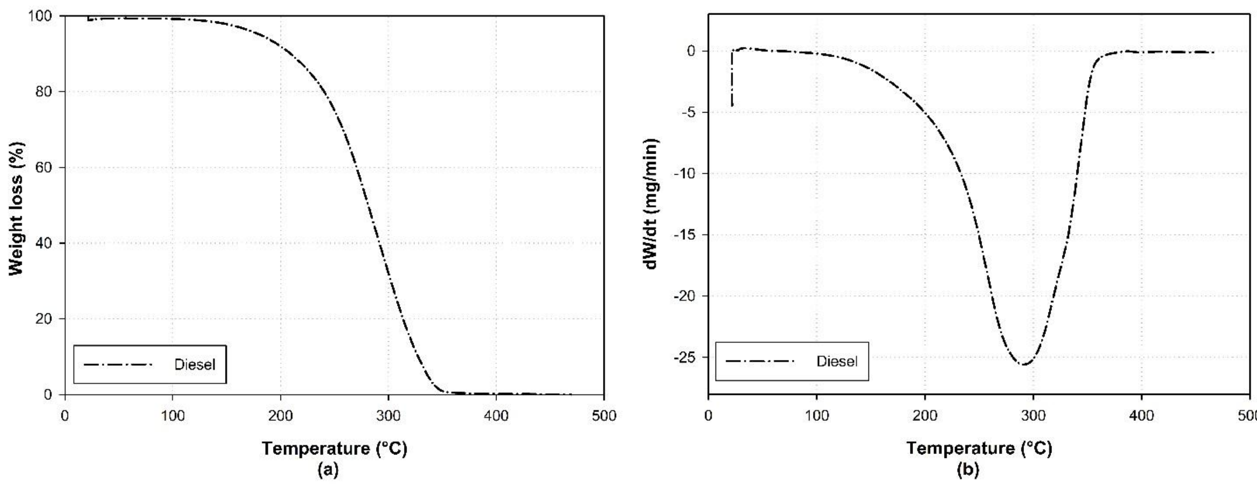

Fig. 2 (a) Thermal gravimetric analysis (TGA), **(b)** Rate of weight loss (dTG) of diesel fuel.

2.2. Experimental test setup

The experimental test setup is represented by the block diagram shown in Figure 3. A single-cylinder compression ignition engine, whose specifications are listed in Table 3, is coupled with a DC electric generator. The power generated is consumed by electric heaters, which act as a load. The power generated is controlled by altering the excitation voltage via a variac transformer. Diesel stored in the fuel tank is used during the engine warming-up phase, and then the fuel line is switched to a diesel graduated burette to allow for fuel volumetric flow rate measurement. Air volumetric flow rate is measured from the differential pressure signal sent to a DAQ NI PCI-6251 data acquisition from a laminar flow element preceding the air damping box. HHO gas is introduced to the intake air from a port in the intake manifold. Temperatures of the exhaust gases, cylinder wall, air box, and ambient air are measured by type K thermocouples. Hoses of the gas analyzer and smoke chamber are connected to the exhaust pipe downstream the exhaust gases flow to measure pollutant concentration and smoke opacity as a soot index. Multimeters measure the output voltage and current that the resistors consume to calculate the output power. The engine rotational speed is set and observed to remain constant using a digital tachometer. The measurement devices used during the experiments are listed in Table 4.

The engine was initially started up and set to a constant rotational speed of 1500 rpm, then left to warm up for 15 minutes, running only on diesel fuel until steady-state temperatures were reached. Measurements of air flow rate, fuel flow rate, temperatures, emissions, power output, and smoke opacity were taken for zero load. The engine load was increased by changing the excitation voltage, and the same process was repeated for 25, 50, 75, and 100% loads. The same experiment was duplicated by adding a 0.25 LPM flow rate of HHO gas generated by the dry cell to the intake manifold of the engine. The experimental program summary is stated in Table 5.

The uncertainty analysis was calculated via the Holman formula [16]. Systematic uncertainties (U_s) provided by the manufacturer, random uncertainties (U_r), and total uncertainties (U_t) are tabulated in Table 6. Random uncertainties were calculated through three consecutive measurements for each variable, with the standard deviation (SD) calculated afterwards [17][18].

$$U_r(\%) = \pm \frac{\left(t * \frac{SD}{\sqrt{N}}\right)}{(X_m)} * 100 \quad \textbf{(1)}$$

where X_m represents the arithmetic mean value for the three consecutive measurements, and t is the student's statistical value equivalent to 1.96 for a 95% confidence level.

The total uncertainties (U_t) are assessed by the following equation.

$$U_t = \pm\sqrt{U_r^2 + U_s^2} \quad \textbf{(2)}$$

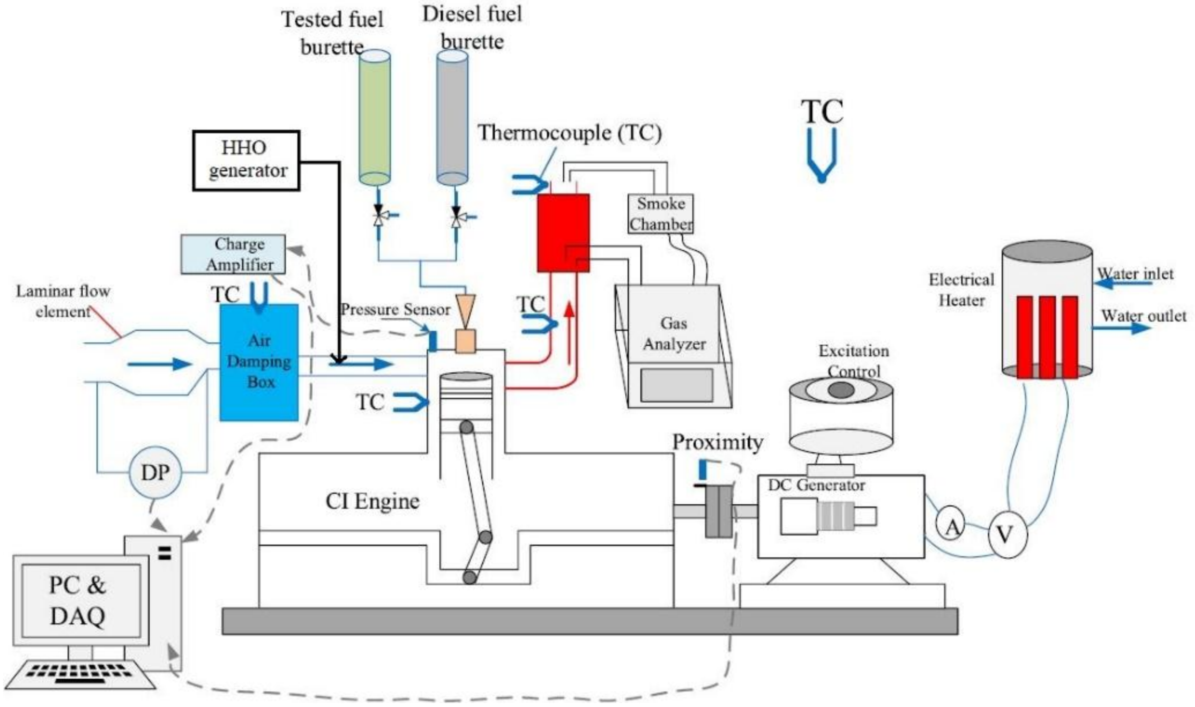

Fig. 3 Experimental setup.

Table 3 Test engine specifications.

Variable	Specification
Engine model	Deutz F1L511
Number of cylinders	1
Aspiration	Natural Aspiration
Cylinder volume	824 cc
Bore diameter	100 mm
Stroke lenght	105 mm
Cooling type	Air cooling
Compression ratio	17:1
Timing of injection	-24˚CA
Injection pressure	175 bar
Pump type	Diaphragm pump
Max. torque	44 N.m at 900 rpm
Rated power	5.7 kW

Rated speed	1500 rpm

Table 4 Measurement devices.

Measured value	Measurement device	Device range (Unit)
Fuel flow rate	A graduated cylinder and a timer	0:100 (mL)
Air flow rate	Setra 239 Diff. pressure transducer MERIAM 50MC2 Laminar flow element device	0:1.245 (kPa) 0:11.3 (m^3/min)
Air and exhaust temperatures	Type K calibrated thermocouples	-200:1370 (˚C)
Smoke opacity	AVL DiSmoke 4000 opacity chamber	0:100%
Exhaust emissions (Electrochemical NO_x sensor, and NDIR CO and UHC sensors)	ECOM-J2KKN-Pro gas analyzer	0:5000 (ppm), 0:6.3 (vol%), 0:4 (vol%)
Engine speed	Omega HHT13 tachometer	0.5:20000 rpm

Table 5 Experimental program summary.

Experiment conditions		Measured Parameters	Calculated parameters
Variable	**Value**		
Engine speed	1500 rpm	• Cylinder pressure versus crank angle • Power output • Fuel consumption • Exhaust emissions concentrations: CO (ppm), NO_x (ppm), UHC (ppm), CO_2 (%), O_2 (%), H_2 (%) • Smoke opacity (%) • Exhaust gases temperature • Ambient air temperature • Air flow rate	• Brake thermal efficiency (BTE) • Brake specific fuel consumption (BSFC) • Air-to-fuel ratio (A/F)
Engine load	0, 25, 50, 75, 100% loads (BMEP of 0, 1.28, 2.58, 4, 4.65 bar).		
Tested fuels	• Diesel • Diesel + 0.25 LPM HHO		

Table 6 Uncertainty and error analysis.

Measured parameter	Systematic uncertainty (U_s)	Random uncertainty (U_r)	Total uncertainty (U_t)
Temperatures	± 1 ˚C	± 0.45 %	± 0.46
Fuel flow rate	± 0.1 mL	± 0.9 %	± 0.91
Air flow rate	± 1 % FSO	± 0.85 %	± 1.31
Differential pressure	± 0.1 % FSO	± 0.75 %	± 1.25
Engine rotational speed	0.2 % FSO	± 0.35 %	± 0.4
Brake power (BP)	1.1 % FSO	± 0.65 %	± 1.28
BSFC	1.4 % FSO	± 0.55 %	± 1.5
Smoke opacity	0.1 % FSO	± 0.7 %	± 0.7
CO	0.1 % FSO	± 0.51 %	± 0.52
NO_x	0.2 % FSO	± 0.5 %	± 0.54

3. Results and discussion

3.1. Performance

The performance characteristics of the dual-fuel test engine run on diesel with and without adding 0.25 LPM HHO modes are discussed in the following section.

3.1.1. Brake thermal efficiency (BTE)

The diesel-fueled engine shows an improvement in brake thermal efficiency while increasing the load, except for the full load conditions, which showed a sudden decline. Introducing the HHO gas to the dual fuel CI engine displays an increase in the brake thermal efficiency for all various loads, including the full load, compared to a diesel-fueled engine with a maximum improvement of 2.13% at full load (BMEP=4.65 bar) as shown in Figure 4 (a). This increment in BTE can be attributed to the higher energy content of the combustible mixture and the higher oxygen content when HHO was added, leading to improved air-fuel mixing and oxidation rates [19].

3.1.2. Brake specific fuel consumption (BSFC)

Figure 4 (b) demonstrates the impact of introducing HHO gas on the BSFC of the test engine, which is defined as the ratio of the consumed fuel mass to the energy produced. For diesel-only test conditions, BSFC decreased as the engine load increased, except for a slight growth in full load conditions. Introducing HHO gas as a supplementary fuel diminished BSFC for all different loads, including full load, with a maximum reduction of 8.75% at full load (BMEP=4.65 bar).

These results match and validate the previous brake thermal efficiency results due to higher oxygen and energy content.

3.1.3. Exhaust gas temperature (EGT)

Figure 5 (a) displays the variation of the exhaust gas temperature (EGT) versus the BMEP of the engine. EGT increased with the engine load increment. Adding HHO caused a significant reduction in the EGT for all loads with a maximum percentage of 4.37% at 75% load (BEMP=4 bar), except for the no-load condition, which shows nearly the same temperature. The decreased rich combustion zone might cause this reduction in EGT by the addition of HHO gas in the diffusion combustion phase and advanced peak pressure towards the compression top dead center, leading to lower exhaust temperature. It should lead to a higher engine efficiency for different loads than the neat diesel combustion mode, as shown previously in the BTE analysis [20][21].

3.1.4. Air-to-fuel ratio (A/F)

The variation of the A/F ratio of the combustible mixture with the BMEP representing each load is shown in Figure 5 (b). The A/F ratio meaningfully decreased while increasing the engine load for all tested fuels. Introducing HHO gas to the combustible charge increases the A/F ratio, reducing the equivalence ratio for all load conditions with a maximum increment percentage for the A/F ratio of 10.68% at full load (BMEP=4.65 bar). This could be attributed to the oxygen content of HHO, which is the main constituent of ambient air, leading to a leaner mixture which should result in assurance of a complete combustion process, a higher thermal efficiency as discussed previously, and a reduction in carbon monoxide (CO) emissions, as would be addressed in the following section [22].

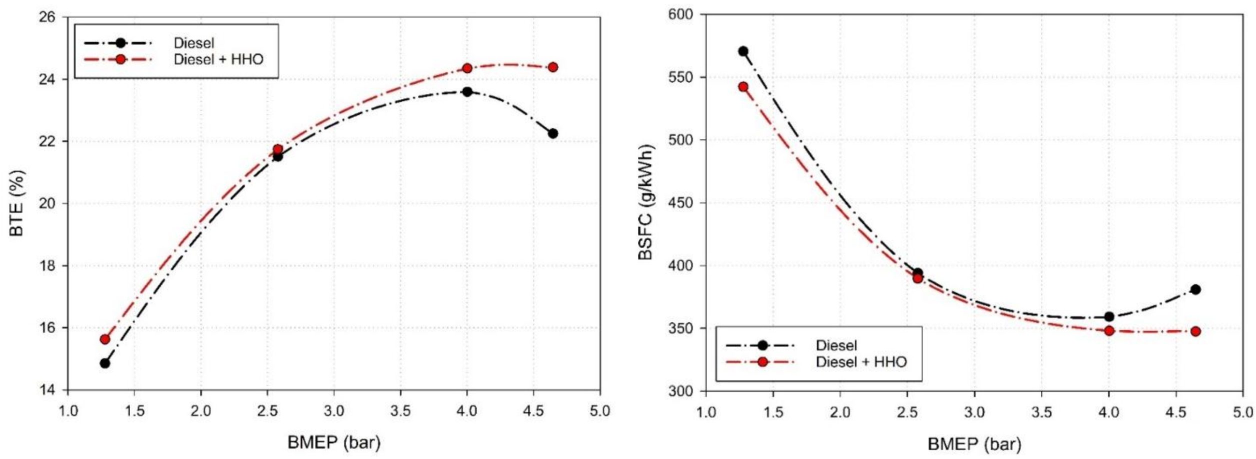

(a) **(b)**

Fig. 4 (a) Variation of BTE with BMEP **(b)** Variation of BSFC with brake mean effective pressure.

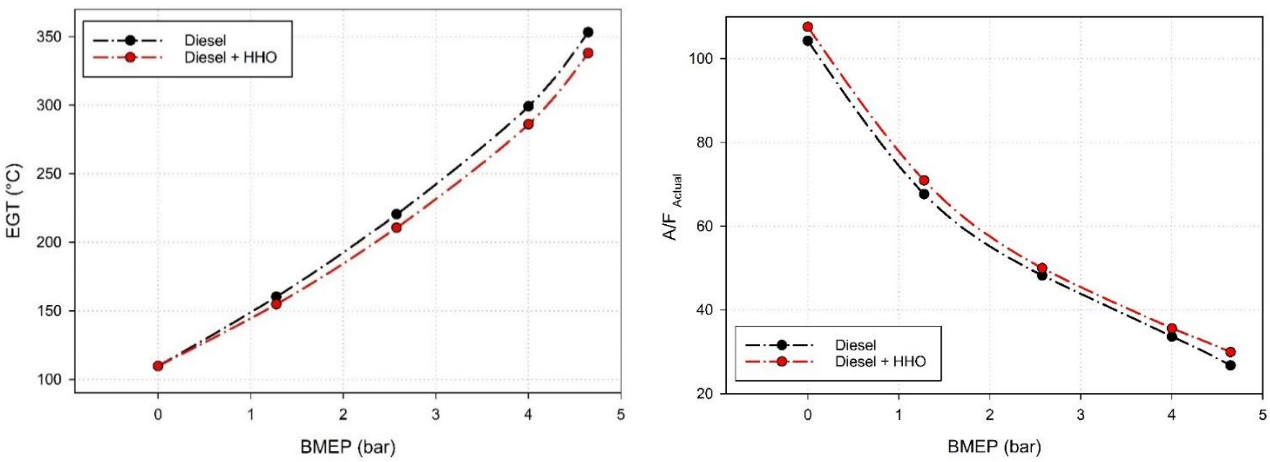

(a) **(b)**

Fig. 5 (a) Exhaust gas temperature at different BMEP of various loads **(b)** Air-to-fuel ratio of tested fuels against BMEP of different loads.

3.2. Emissions

The emissions characteristics of the dual fuel test engine run on both diesel with and without adding 0.25 LPM HHO modes are discussed in the following section:

3.2.1. Carbon monoxide (CO)

Carbon monoxide (CO) concentration in exhaust gases for different tests is shown in Figure 6 (a). CO level decreased for low engine loads until it dramatically increased for high engine loads to higher concentrations. This could occur due to the increased CO oxidation rate at higher temperatures for low and medium loads. Then, at high loads, higher fuel amounts in the combustion chamber lead to a deficiency of oxygen, which causes incomplete combustion, leading to a higher rate of CO emissions at high loads [23]. Introducing HHO to the combustible diesel and air mixture in the dual fuel engine mode led to a similar CO concentration for low engine loads and a substantial decrease of CO concentration for high engine loads compared to diesel combustion mode, with a maximum decrement of 31.8% at full load (BMEP=4.65 bar). This can be attributed to the higher cetane number and the oxygen content of the HHO gas, which enhances the complete combustion process and elevates the oxidation rate of CO.

3.2.2. Carbon dioxide (CO_2)

The variation of CO_2 as a percentage of the exhaust emissions versus the brake mean effective pressure of the engine is shown in Figure 6 (b). The CO_2 percentage generally increases as the engine load increases due to the escalated fuel amount delivered to the combustion chamber, which increases emission levels [24]. HHO and diesel combustion mode slightly decreased CO_2 emissions for no load and high load conditions, with a comparable percentage for the rest of the engine load range compared to diesel combustion mode. The maximum diminishment was by 0.18% at 75% load (BMEP=4 bar). These close results can be attributed to the effect of the two contradictory parameters: the decreased fuel consumption of the engine when HHO was introduced, causing less exhaust emissions, and the increased oxidation rate of CO to CO_2 as the oxygen content in HHO enhances the complete combustion.

3.2.3. Nitrogen oxides (NO_x)

Figure 7 (a) shows the variation of nitrogen oxides (NO_x) against different engine loads represented in brake mean effective pressures of each load. NO_x emissions increase with the increment of the engine load for the diesel combustion mode. This may be caused by the lower combustion speed of the leaner air-fuel mixtures as the load increases, which leads to increased NO_x emissions. Introducing HHO to the engine in dual fuel combustion mode significantly reduces NO_x emissions across the entire range of engine loads. The maximum NO_x reduction percentage was 8.34% against 75% load (BMEP=4 bar). These drops in NO_x levels can be attributed to lower peak combustion pressure, shorter combustion duration, and lower combustion temperature due to the cooling effect of HHO gas [24].

3.2.4. Unburned hydrocarbons (UHC)

Unburned hydrocarbons (UHC) result from fuel incomplete combustion. UHC concentration against different loads is plotted in Figure 7 (b). It can be indicated that UHC formation increases as engine load increases. The introduction of HHO gas in dual fuel mode caused a substantial diminishment of UCH formation at all various loads, with a maximum reduction percentage of 12.4% at 75% load (BMEP=4 bar). This is attributed to the rich oxygen content of HHO gas, which enhances the oxidation process and complete combustion [23].

3.2.5. Smoke opacity

Figure 8 shows an increase in smoke opacity while increasing engine load. This occurs due to the large phase of diffusion combustion at high loads as soot formation grows at the fuel-rich zones of the diffusion flame. Introducing HHO gas in dual fuel mode causes a noticeable decrease in smoke opacity compared to diesel mode for all loads represented in brake mean effective pressure. The maximum diminishment was 4.4% at full load (BMEP=4.65 bar). This reduction can be related to the higher oxygen level of HHO gas, which improves the oxidation process, resulting in less emitted soot [24].

3.2.6. Oxygen (O_2)

O_2 exhaust concentration generally decreases as engine load increases for diesel combustion in CI engines, as shown in Figure 9 (a). This decline at higher loads is due to the higher fuel amount available in the combustion chamber, leading to oxygen deficiency [23]. Including HHO gas in dual combustion mode caused a noticeable rise in O_2 emissions for all tested engine loads compared to neat diesel mode, with a maximum value of 0.7% at full load (BMEP=4.65 bar). This increase is due to the oxygen content in the added HHO gas.

3.2.7. Hydrogen (H_2)

Figure 9 (b) shows the variation of H_2 concentrations in the exhaust emissions versus the brake mean effective pressure of the engine. H_2 concentration is generally zero for all engine loads except for high loads for the diesel mode. Introducing HHO to the combustible mixture in dual fuel mode led to a significant increase in H_2 concentration for low engine loads with a tapering increment percentage as the engine is loaded, until a reduction of H_2 was observed at full load by 9.5%. This declining increment can be attributed to the hydrogen content of the introduced HHO gas, which was plenty for low and medium engine loads, but on the other hand, it can be noted from the reduction of the hydrogen content at full load that the engine was still capable of consuming higher HHO flow rates at the full load condition.

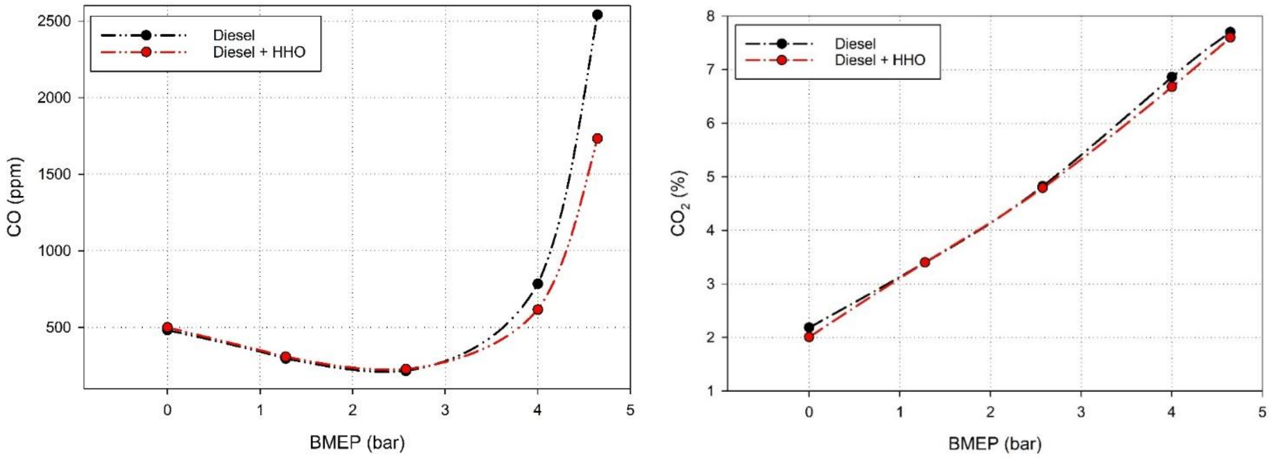

(a) **(b)**

Fig. 6 (a) CO emissions against different BMEP **(b)** CO_2 emissions for different BMEP.

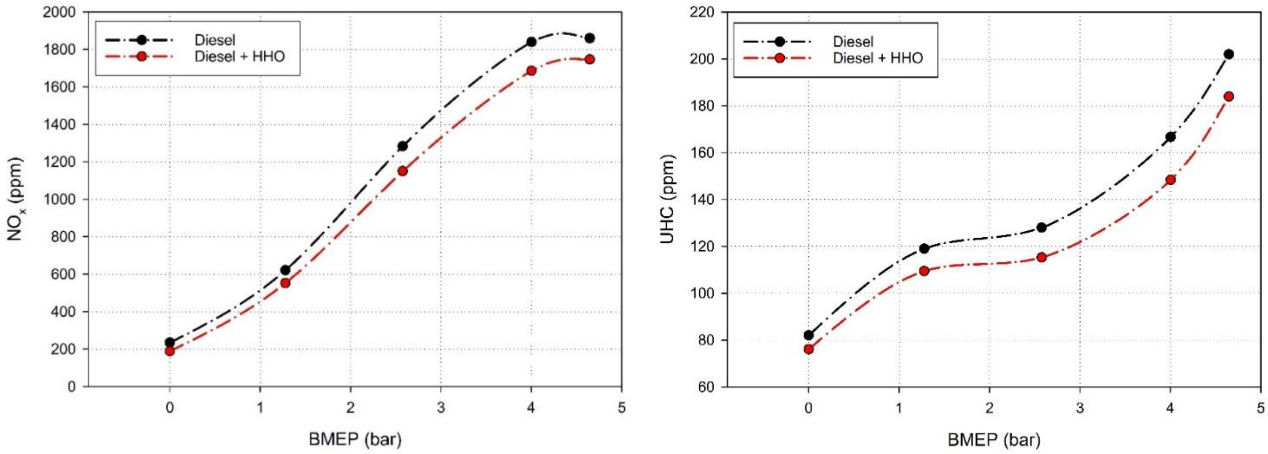

(a) **(b)**

Fig. 7 (a) NO_x emissions for different BMEP **(b)** Unburned hydrocarbons (UHC) for various BMEP.

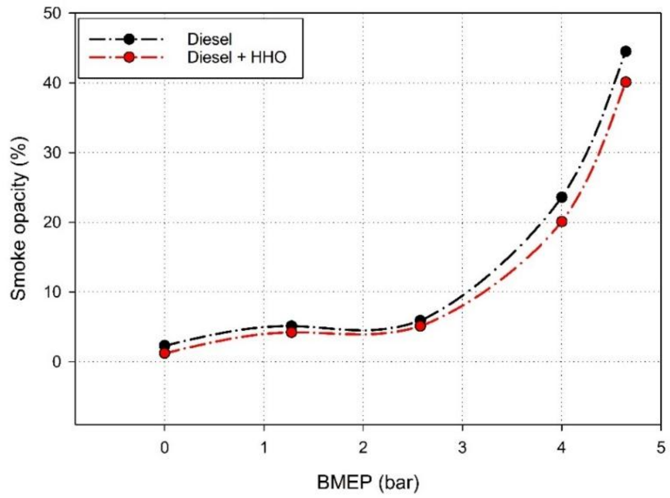

Fig.8 Smoke opacity against different BMEP of engine loads.

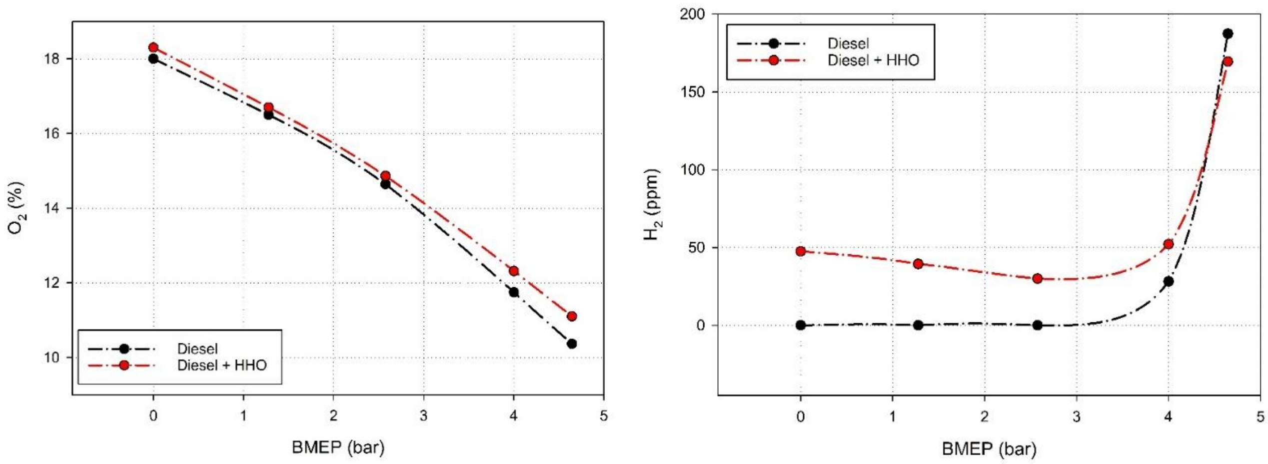

(a) **(b)**

Fig. 9 (a) O_2 emissions for different BMEP **(b)** H_2 concentration in emissions against BMEP**.**

4. Conclusions

This study examined the physical characteristics of oxyhydrogen gas (HHO) as an enrichment fuel for compression ignition (CI) engines and its associated electrolyzers. Various parameters, including cell type, electrolysis current, voltage, plate number and dimensions, and electrolyte concentration, influenced HHO gas production. A dry cell electrolyzer capable of producing up to 1.75 liters per minute (LPM) of HHO was designed and implemented. A single-cylinder dual-fuel diesel engine's performance and emissions characteristics were evaluated under two operating modes: fueled by neat diesel only and fueled by diesel supplemented with a constant 0.25 LPM flow rate of HHO gas. Performance analysis revealed that the introduction of HHO enhanced brake thermal efficiency (BTE) and air-to-fuel ratio (A/F), while reducing brake-specific fuel consumption (BSFC) and exhaust gas temperature (EGT). Emission results demonstrated reductions in carbon monoxide (CO), unburned hydrocarbons (UHC), nitrogen oxides (NO_x), and smoke opacity, an indicator of soot formation. Oxygen and hydrogen levels increased during dual-fuel combustion, whereas carbon dioxide (CO_2) emissions remained essentially unchanged, except for minor reductions at full load and no-load conditions.

For future research, it is recommended that higher HHO flow rates be tested on CI diesel-fueled engines to identify the optimal enrichment ratio based on engine size and injection type. Additionally, the significant emissions improvements achieved with HHO make it a promising supplementary fuel for biodiesels with suboptimal emission profiles, potentially reducing their overall environmental impact.

Acknowledgment

The experimental program of this research was completely conducted at the combustion and environmental labs of Benha Faculty of Engineering, Benha University, Egypt.

References

[1] Kanimozhi B, Kumar G, Alsehli M, Elfasakhany A, Veeman D, Balaji S, et al (2022). Effects of oxyhydrogen on the CI engine fueled with the biodiesel blends: A performance, combustion and emission characteristics study. Int J Hydrogen Energy 2022;47:37668–76. doi:10.1016/j.ijhydene.2021.08.054.

[2] Sadek Mohamed Hassan (2023). Thermal combustion characteristics of stabilized swirl burner for Prevaporized Partially Premixed Flames. Benha J Appl Sci 2023;8:293–304. doi:10.21608/bjas.2023.202962.1139.

[3] G. Elmoslimany A, Soliman Huzayyin A, M. Saadeldin Eldalil K (2022). Performance Improvement of Wells Turbine Using Variable Shaped Blades. Benha J Appl Sci 2022;7:155–61. doi:10.21608/bjas.2022.375729.

[4] Baltacioglu MK, Kenanoglu R, Aydın K (2019). HHO enrichment of bio-diesohol fuel blends in a single cylinder diesel engine. Int J Hydrogen Energy 2019;44:18993–9004. doi:10.1016/j.ijhydene.2019.02.060.

[5] Yilmaz AC, Uludamar E, Aydin K (2010). Effect of hydroxy (HHO) gas addition on performance and exhaust emissions in compression ignition engines. Int J Hydrogen Energy 2010;35:11366–72. doi:10.1016/j.ijhydene.2010.07.040.

[6] Paparao J, Murugan S (2021). Oxy-hydrogen gas as an alternative fuel for heat and power generation applications - A review. Int J Hydrogen Energy 2021;46:37705–35. doi:10.1016/j.ijhydene.2021.09.069.

[7] Ismail TM, Ramzy K, Abelwhab MN, Elnaghi BE, Abd El-Salam M, Ismail MI (2018). Performance of hybrid compression ignition engine using hydroxy (HHO) from dry cell. Energy Convers Manag 2018;155:287–300. doi:10.1016/j.enconman.2017.10.076.

[8] EL-Seesy AI, Aboukhalifa M (2024). Chapter

15 - Oxyhydrogen production and optimization using electrolysis and its application in engines. In: Abd-Elsalam KA, Shankar MVBT-N for HP and S, editors., Elsevier; 2024, p. 389–424. doi:https://doi.org/10.1016/B978-0-443-21456-1.00007-2.
[9] El Soly AK, El Kady MA, Farrag AEF, Gad MS (2021). Comparative experimental investigation of oxyhydrogen (HHO) production rate using dry and wet cells. Int J Hydrogen Energy 2021;46:12639–53. doi:10.1016/j.ijhydene.2021.01.110.
[10] Thangaraj S, Govindan N (2018). Investigating the pros and cons of browns gas and varying EGR on combustion, performance, and emission characteristics of diesel engine. Environ Sci Pollut Res 2018;25:422–35. doi:10.1007/s11356-017-0369-4.
[11] Gad MS, Abdel Razek SM (2021). Impact of HHO produced from dry and wet cell electrolyzers on diesel engine performance, emissions and combustion characteristics. Int J Hydrogen Energy 2021;46:22277–91. doi:10.1016/j.ijhydene.2021.04.077.
[12] Liu S, Wang Z, Li XX, Zhao Y, Li RN (2016). Effects on emissions of a diesel engine with premixed HHO. RSC Adv 2016;6:23383–9. doi:10.1039/c5ra27761b.
[13] Abbas Gohar G, Raza H (2017). Comparative Analysis of Performance Characteristics of CI Engine with and without HHO Gas (Brown Gas). Adv Automob Eng 2017;06. doi:10.4172/2167-7670.1000172.
[14] Manu P V., Sunil A, Jayaraj S (2016). Experimental Investigation Using an On-board Dry Cell Electrolyzer in a CI Engine Working on Dual Fuel Mode. Energy Procedia 2016;90:209–16. doi:10.1016/j.egypro.2016.11.187.
[15] Paparao J, Murugan S (2022). Dual-fuel diesel engine run with injected pilot biodiesel-diesel fuel blend with inducted oxy-hydrogen (HHO) gas. Int J Hydrogen Energy 2022;47:17788–807. doi:10.1016/j.ijhydene.2022.03.235.
[16] Holman JP (1994). Experimental methods for engineers. 1994;9. doi:10.1016/0894-1777(94)90118-X.
[17] Moffat RJ (1988). Describing the uncertainties in experimental results. Exp Therm Fluid Sci 1988;1:3–17. doi:https://doi.org/10.1016/0894-1777(88)90043-X.
[18] Hawwash AA, Mori S, Hassan H (2023). An experimental investigation on the performance of designed closed reactor system on the thermochemical heat storage of magnesium chloride hexahydrate. Exp Heat Transf 2023;00:1–20. doi:10.1080/08916152.2023.2240807.
[19] Wang X, Ni P (2017). Combustion and emission characteristics of diesel engine fueled with diesel-like fuel from waste lubrication oil. Energy Convers Manag 2017;133:275–83. doi:10.1016/j.enconman.2016.12.018.
[20] Sadhik Basha J, Anand RB (2014). Performance, emission and combustion characteristics of a diesel engine using Carbon Nanotubes blended Jatropha Methyl Ester Emulsions. Alexandria Eng J 2014;53:259–73. doi:10.1016/j.aej.2014.04.001.
[21] Thangaraj S, Govindan N (2018). Evaluating combustion, performance and emission characteristics of diesel engine using karanja oil methyl ester biodiesel blends enriched with HHO gas. Int J Hydrogen Energy 2018;43:6443–55. doi:10.1016/j.ijhydene.2018.02.036.
[22] EL-Seesy AI, Waly MS, He Z, El-Batsh HM, Nasser A, El-Zoheiry RM (2021). Influence of quaternary combinations of biodiesel/methanol/n-octanol/diethyl ether from waste cooking oil on combustion, emission, and stability aspects of a diesel engine. Energy Convers Manag 2021;240:114268. doi:10.1016/j.enconman.2021.114268.
[23] Uyumaz A (2020). Experimental evaluation of linseed oil biodiesel/diesel fuel blends on combustion, performance and emission characteristics in a DI diesel engine. Fuel 2020;267:117150. doi:10.1016/j.fuel.2020.117150.
[24] EL-Seesy AI, El-Zoheiry RM, Ali MIH (2025). Recycling of waste lubricant oil using two-step pyrolysis to produce fuel-like diesel and enhancing its combustion and emission parameters in diesel engines using linseed biodiesel. Energy Convers Manag X 2025;26:100924. doi:10.1016/j.ecmx.2025.100924.